Hindawi Publishing Corporation
Journal of Nanotechnology
Volume 2011, Article ID 506862, 6 pages
doi:10.1155/2011/506862

Research Article

Bimetallic Pt-Ru Nanoparticle Catalyst for Hydrogen Peroxide Detection

Metini Janyasupab,[1] Yuan Zhang,[2] Po-Yuan Lin,[3] Brandon Bartling,[1] Jiaqiang Xu,[2] and Chung-Chiun Liu[1]

[1] *Department of Chemical Engineering, Case Western Reserve University, Cleveland, OH 44106, USA*
[2] *Department of Chemistry, Shanghai University, Shanghai 200444, China*
[3] *Department of Material Sciences and Engineering, Case Western Reserve University, Cleveland, OH 44106, USA*

Correspondence should be addressed to Metini Janyasupab, mxj52@case.edu

Received 10 June 2011; Revised 3 August 2011; Accepted 4 August 2011

Academic Editor: Charles M. Lukehart

A bimetallic Pt-Ru nanoparticle catalyst was prepared and characterized for the enhancement of hydrogen peroxide (H_2O_2) detection in biosensing applications. The particles were synthesized via sodium borohydride reduction, with low heat treatment, and characterized by TEM and HRTEM. The chemical composition analyses were performed by EDX. The bimetallic particle diameters ranged from 2 to 12 nm, with an average of 4.5 nm. The Pt-Ru catalyst exhibited an improved performance at low overpotential (+0.2 V versus Ag/AgCl reference electrode) in H_2O_2 detection, suggesting a sensitivity value of 78.95 $\mu A \cdot mM^{-1}$ (or 402.1 $\mu A \cdot mM^{-1} \cdot cm^{-2}$) which was 30% higher than that for the single Pt catalyst. The major contribution of this enhancement comes from the stronger oxygen adsorption on Ru metal. The Pt-Ru catalyst also showed a more stable signal at the high overpotential (+0.4 V versus Ag/AgCl), providing better accuracy in the detection of H_2O_2.

1. Introduction

Measuring hydrogen peroxide (H_2O_2) is important as an indicator in many enzymatic reactions [1–4]. Its deviation from a normal metabolic condition is an indicator of cell function failures. For example, the deficit of insulin is often related to the lower level H_2O_2, due to a decrease in the glucose conversion process [5, 6]. Clark and Lyons [7] demonstrated the electrochemical oxidation of H_2O_2 from the glucose oxidase enzymatic reaction that nowadays is commonly used for diabetic diagnosis and management. Furthermore, the other enzymatic reactions that produce H_2O_2 can also be used to quantify the analytes by the same principle as glucose oxidation. Therefore, the detection of H_2O_2 by electrochemical oxidation is important.

Metal catalysts such as platinum, palladium, gold, or iridium [8–13] are often used for H_2O_2 biosensing applications. Based on the theoretical trend and simulation studies [14–18], Ru apparently requires less activation energy than Pt to adsorb OH_{ads} as well as O_{ads}. Gsell and coworkers [19, 20] reported that the oxygen adsorption preferably occurred onto the Ru (0001), hcp, surface. This observation may allow the O_{ads} inhibitor to interact with Ru metal, thereby minimizing the side reactions to poison the Pt metal. Consequently, Pt active binding sites may have a higher possibility of interacting with H_2O_2, enhancing the catalytic activity of the H_2O_2 detection.

In our research, the Pt-Ru nanoparticles were synthesized by using sodium borohydride reduction. Material characterization was assessed by using TEM and EDX to examine the structural property and verify elemental composition, respectively. For electrochemical performance, the detection of H_2O_2 was performed on a 5% wt. Pt-Ru catalyst working electrode and experimentally assessed by amperometry. Our study demonstrated that the Pt-Ru catalyst shows a significantly higher sensitivity of amperometric current at an overpotential of +0.2 V versus Ag/AgCl, and a more stable signal at +0.4 V overpotential than that for the single Pt and single Ru.

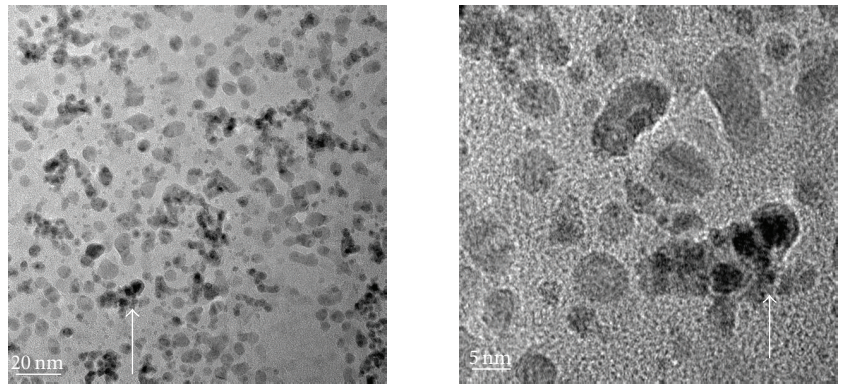

(a) (b)

Figure 1: TEM (a) and HRTEM (b) of Pt-Ru nanoparticles in aqueous colloid; the arrows denote the same location.

2. Experimental

2.1. Chemical Materials for the Synthesis. Hydrogen hexachloroplatinate (IV) hexahydrate ($H_2PtCl_6 \cdot 6H_2O$, 37.5% Pt basis), ruthenium (III) chloride hydrate ($RuCl_3 \cdot nH_2O$, 99.8% purity) were used as precursors for the Pt and Ru metal nanoparticles, respectively. Citric acid (99.5 wt.%) and sodium borohydride ($NaBH_4$, 99 wt.%) were prepared as the capping and reducing agent, respectively. The pH of the solution was adjusted by sodium hydroxide solution. All chemicals were purchased from Sigma Aldrich (St. Louis, MO) and used as received without further purification. Vulcan XC 72 carbon black (Cabot, Boston, MA) was used as a supporting material. Nafion solution (LIQUION) was purchased from Ion Power Inc., New Castle, DE.

2.2. Preparation of Pt-Ru Nanoparticle Catalyst. The Pt-Ru was synthesized via the borohydride reduction as published by Shimazaki et al. [21] with the following modifications: the Pt and Ru precursors were dissolved separately in deionized (DI) water achieving a 1.8 mM metal solution. 5.55 mL of both Pt and Ru solution (for Pt-Ru, 1 : 1 ratio) was added together to obtain a 0.01 M bimetallic Pt-Ru solution. The citric acid was added to prevent particle agglomeration at a molar ratio of citric acid to the metal solution of 0.42. The bimetallic Pt-Ru solution was then adjusted to pH = 7.0 by 0.1 M NaOH solution. Finally, the nanoparticle solution was then added dropwise by the amount of $NaBH_4$ 1.4-times the theoretical value of the number of electron required to reduce the metal solution. The solution was stirred overnight for the completion of the chemical reduction. For nanoparticle carbon-paste catalyst preparation, the Pt-Ru solution was sonicated for 30 minutes, and the active carbon black powder Vulcan XC was then added. The catalyst solution was stirred overnight, removing the liquid by centrifugation and was then dried at 50°C in vacuum for 12–20 hours.

2.3. Material Characterization. Transmission electron microscopy (TEM) and high-resolution TEM (HRTEM) images were obtained by *Techai F30* FEI with the high accelerating voltage of 300 keV. The TEM samples of Pt, Pt-Ru, and Ru nanoparticle solution had initially undergone sonication for 3 hours. A droplet of the solution was deposited onto an ultrathin carbon-copper grid (Ted Pella, Inc., Redding CA) and dried at room temperature. The chemical composition and elemental mapping were performed in the same sample by energy dispersive X-ray spectroscopy (EDX).

2.4. Electrochemical Testing. Amperometric studies were carried out. A glassy carbon rotational disk electrode (RDE, diameter of 5 mm.) and the Electrochemical Workstation, Model 660 C, CH Instrument (Austin, TX) were used. 8 mg of 5% wt. Pt-Ru nanoparticle catalyst was grounded and mixed with ethanol (200 μL). Then, 4 μL of this catalytic solution was deposited onto a glassy carbon electrode and dried at room temperature for 10 minutes. Finally, a 4 μL of 5 wt.% Nafion solution was then deposited on top of the electrode and dried for another 10 minutes in open air. Prior to the experiment, the electrode was washed thoroughly with isopropanol and acetone in sequence, then polished by 0.05 μm aluminum powder solution and sonicated for 10 minutes to remove any remaining residue. A three-electrode system of a Pt counter electrode, an Ag/AgCl reference electrode, and a glassy carbon working electrode was employed for the amperometric studies. The working electrode was operated at a rotational speed 900 rpm, which was determined to adequately maintain the hydraulic effect. Testing samples were performed in 0.1 M PBS at pH 7.2 with 0.15 M KCl as supporting electrolyte.

3. Results and Discussion

3.1. Structure and Cluster Size. Figures 1–3 show typical TEM images of Pt-Ru, Pt, and Ru nanoparticles in aqueous solution. The structural formation and cluster size of the Pt-Ru appeared different from both the single Pt and the single Ru. As shown in Figure 1(a), the bimetallic cluster appeared highly dispersed. On the other hand, each single Pt cluster connected to its neighboring cluster, forming a

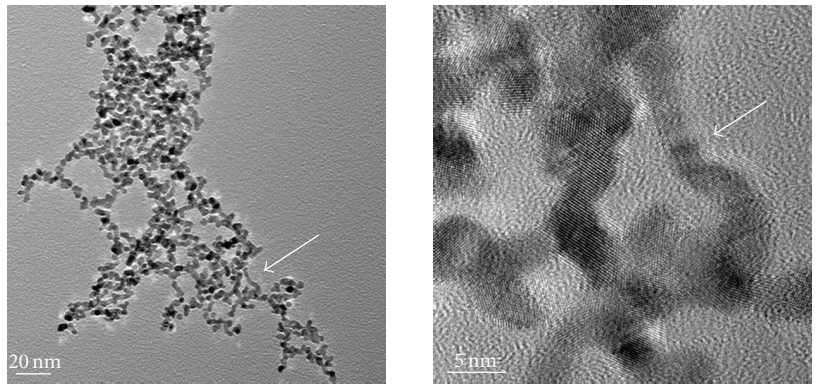

(a) (b)

Figure 2: TEM (a) and HRTEM (b) of Pt nanoparticles in aqueous colloid; the arrows denote the same location.

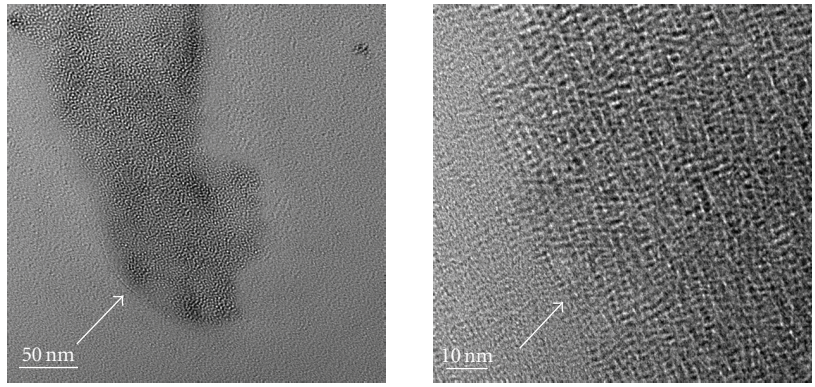

(a) (b)

Figure 3: TEM (a) and HRTEM (b) of Ru nanoparticles in aqueous colloid; the arrows denote the same location.

branch-like network as seen in Figure 2(a). In spite of the different structural formation, the single Pt had a similar particle size to that of Pt-Ru. Both of them ranged from 2 to 12 nm, with an average diameter of 4.0 and 4.5 nm for the Pt and the Pt-Ru, respectively.

Furthermore, at a higher resolution of the TEM image (Figure 1(b)), the phase contrast lattice fringes of the Pt-Ru are nearly unnoticeable. In contrast, those lattice fringes found in the single Pt are highly visible as shown in Figure 2(b). More interestingly, the Ru appeared amorphous in Figure 3, suggesting that the less crystalline structure of the Pt-Ru could be contributed to the incorporation of Ru metal in this synthesis.

3.2. Chemical Composition. Chemical compositions of the samples in Figures 1–3 were performed by EDX analysis. As illustrated by Figure 4, the bimetallic nanoparticles revealed all of the peaks that were found in the single Pt and the single Ru at the exact same location. Thus, the elemental mapping of the Pt-Ru confirmed the presence of both metals in the bimetallic sample. In addition to those peaks, there are other elements that are commonly found in this synthesis and preparation. For example, the Na peak and the O peak were caused by the remaining residues in $NaBH_4$ reduction. Also, the Cu and Fe peaks were part of the copper grid and TEM instrument.

3.3. Electrochemical Characterization. Amperometry was used to evaluate electrochemical performance on three metallic working electrodes. Prior to an experiment, an open circuit potential was measured to determine the equilibrium potential. Among these three metals, the Pt-Ru working electrode has the open circuit potential of +0.25 V, which was higher than that of the Ru (0.00 V), but lower than the single Pt (+0.30 V) versus Ag/AgCl reference electrode. Because each metal has a different equilibrium potential, overpotential is considered to quantify the actual performance of the metals in the H_2O_2 detection [22]. Thus, two overpotentials of +0.2 and +0.4 V versus Ag/AgCl were arbitrarily selected based on H_2O_2 detecting scheme in physiological fluid. Furthermore, in order to directly relate the contribution of H_2O_2 to the current response, the electrode was operated at 900 rpm to control the diffusion limiting current. Thus, only the catalytic reaction from H_2O_2 contributed to a change of current.

Figure 5 shows the amperometric response of each metallic catalyst at the low overpotential of +0.2 V, and each increasing step of current corresponds to 0, 0.5, 1, 2, 3, 5, 7,

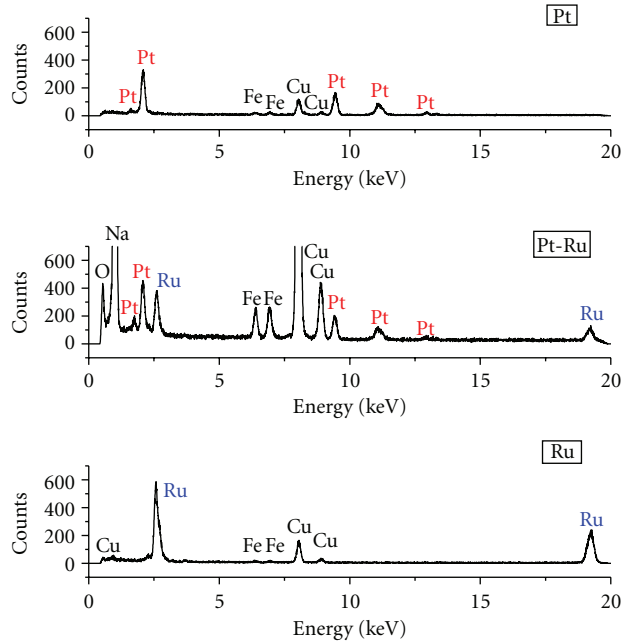

FIGURE 4: EDX characteristic peaks of colloidal Pt, Pt-Ru, and Ru nanoparticles; Fe and Cu corresponding to the instrumental artifact; Na and O corresponding to residues from the synthesis.

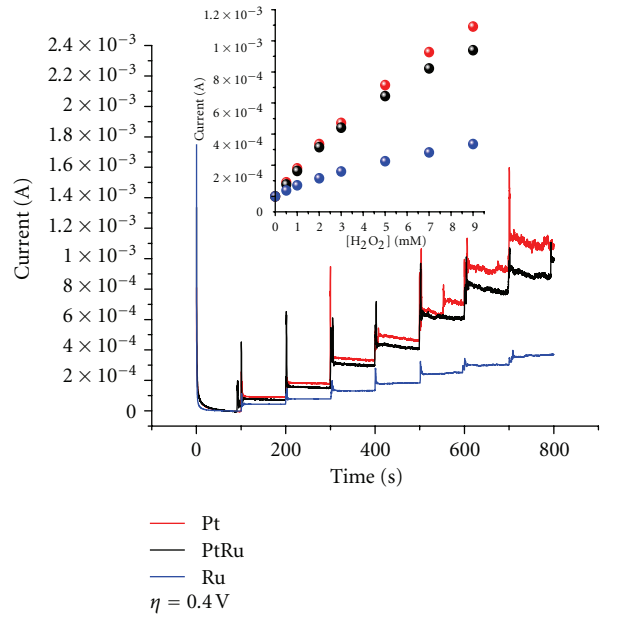

FIGURE 6: Amperometric curves and current-concentration relationship (insert) of Pt (red), Pt-Ru (black), and Ru (blue) for H_2O_2 injections at overpotential of +0.4 V.

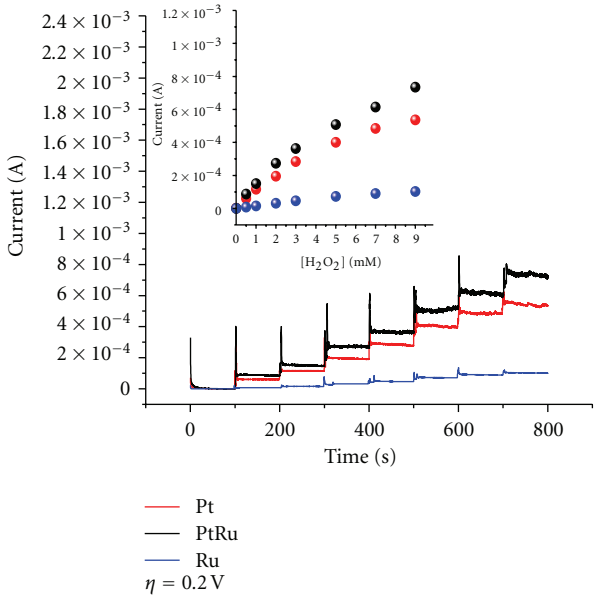

FIGURE 5: Amperometric curves and current-concentration relationship (insert) of Pt (red), Pt-Ru (black), and Ru (blue) for H_2O_2 injections at overpotential of +0.2 V.

and 9 mM H_2O_2. The sensitivity of each metal is evaluated by the steady-state current calibration curve as shown in the insert plot. In particular, the sensitivity of the Pt-Ru was estimated to be 78.95 $\mu A \cdot mM^{-1}$ or 402.1 $\mu A \cdot mM^{-1} \cdot cm^{-2}$ (based on the geometric area) whereas the single Pt and the single Ru have the sensitivity of 59.93 and 11.67 $\mu A \cdot mM^{-1}$, respectively. Therefore, the Pt-Ru catalyst showed superior performance and improved the sensor's sensitivity by 31.7–57.6% when compared to single metallic catalysts.

Figure 6 shows the testing results of the electrode materials shown in Figure 5 but at a higher overpotential of +0.4 V. The sensor sensitivity of the Pt-Ru working electrode was 105.7 $\mu A \cdot mM^{-1}$. Unlike at low overpotential, the bimetallic sensitivity was lower than that of the single Pt by 13.2%. Nevertheless, the Pt-Ru had the smaller standard deviation, indicating a good stability of the electrode at this higher overpotential.

In practical applications, a low oxidation potential to H_2O_2 is preferred for the detection of H_2O_2 to minimize the oxidation of any other chemical species, and our experimental results show that at the low overpotential of +0.2 V, the Pt-Ru working electrode is preferred to detect H_2O_2. According to the bifunctional theory by Watanabe et al. [23], the incorporation of the bimetallic Pt-Ru could minimize the side reactions [24, 25] on Pt catalyst sites. Because Ru required less adsorption energy than Pt, oxygen and proton would be preferably adsorbed by $Ru(OH)_2$. As a result, more H_2O_2 interacted with the Pt active binding sites [26–30], which led to a favorable condition for the oxidation of the H_2O_2 in this case. Hence, the bimetallic catalyst could provide a higher oxidation current output from the H_2O_2 detection, translating to higher sensitivity. However, at a high overpotential of +0.4 V, the adsorption of O species in both metals could increase and form $Pt(OH)_2 \cdot O_2$ and $Ru(OH)_2 \cdot O_2$ poisoning the surface of the electrode. Therefore, the bimetallic catalyst might not be as sensitive as the single Pt metal. Nonetheless, its stability was very good and was favored at this overpotential.

4. Conclusion

The electrochemical performance of the bimetallic Pt-Ru catalyst was investigated for H_2O_2 detection. In our study, we found that the sensitivity of the Pt-Ru was enhanced by 30% when compared to the single Pt. Not only did the Pt-Ru improve the catalytic performance, the smaller concentration of the expensive Pt metal could provide benefits to sensor manufacturing and lead to practical applications in enzymatic determination related to many other H_2O_2-related reactions.

Acknowledgments

This paper study is financially supported by Royal Thai Government Scholar Fellowship, China Scholarship Council Postgraduate Scholarship Program, and the NSF Grant no. 1000768, and a research grant from the Delta Environmental and Educational Foundation is also gratefully acknowledged. Special thanks to Amir Avishai for an enlightening discussion in the TEM and HRTEM analysis assistance.

References

[1] A. Virion, J. L. Michot, and D. Deme, "NADPH-dependent H_2O_2 generation and peroxidase activity in thyroid particular fraction," *Molecular and Cellular Endocrinology*, vol. 36, no. 1-2, pp. 95–105, 1984.

[2] A. Vazquez, J. Tudela, R. Varón, and F. García-cánovas, "A kinetic study of the generation and decomposition of some phenothiazine free radicals formed during enzymatic oxidation of phenothiazines by peroxidase-hydrogen peroxide," *Biochemical Pharmacology*, vol. 44, no. 5, pp. 889–894, 1992.

[3] N. Kiba, Y. Goto, and M. Furusawa, "Simultaneous determination of glucose and 1-deoxyglucose in serum by anion-exchange chromatography with an immobilized pyranose oxidase reactor," *Journal of Chromatography—Biomedical Applications*, vol. 620, no. 1, pp. 9–13, 1993.

[4] Z. Rosenzweig and R. Kopelman, "Analytical properties and sensor size effects of a micrometer-sized optical fiber glucose biosensor," *Analytical Chemistry*, vol. 68, no. 8, pp. 1408–1413, 1996.

[5] U. Wollenberger, V. Bogdanovskaya, S. Bobrin, F. Scheller, and M. Tarasevich, "Enzyme electrodes using bioelectrocatalytic reduction of hydrogen peroxide," *Analytical Letters*, vol. 23, no. 10, pp. 1795–1808, 1990.

[6] A. Heller, "Implanted electrochemical glucose sensors for the management of diabetes," *Annual Review of Biomedical Engineering*, vol. 1, no. 1, pp. 153–175, 1999.

[7] L. C. Clark and C. Lyons, "Electrode systems for continuous monitoring in cardiovascular surgery," *Annals of the New York Academy of Sciences*, vol. 102, pp. 29–45, 1962.

[8] Y. Zhang and G. S. Wilson, "Electrochemical oxidation of H2O2 on Pt and Pt + Ir electrodes in physiological buffer and its applicability to H2O2-based biosensors," *Journal of Electroanalytical Chemistry*, vol. 345, no. 1-2, pp. 253–271, 1993.

[9] H.-W. Lei, B. Wu, C.-S. Cha, and H. Kita, "Electro-oxidation of glucose on platinum in alkaline solution and selective oxidation in the presence of additives," *Journal of Electroanalytical Chemistry*, vol. 382, no. 1-2, pp. 103–110, 1995.

[10] S. S. Razola, B. L. Ruiz, N. M. Diez, H. B. Mark, and J. M. Kauffmann, "Hydrogen peroxide sensitive amperometric biosensor based on horseradish peroxidase entrapped in a polypyrrole electrode," *Biosensors and Bioelectronics*, vol. 17, no. 11-12, pp. 921–928, 2002.

[11] X. Xu, S. Liu, and H. Ju, "A novel hydrogen peroxide sensor via the direct electrochemistry of horseradish peroxidase immobilized on colloidal gold modified screen-printed electrode," *Sensors*, vol. 3, no. 9, pp. 350–360, 2003.

[12] S. Hui, J. Zhang, X. Chen et al., "Study of an amperometric glucose sensor based on Pd-Ni/SiNW electrode," *Sensors and Actuators, B*, vol. 155, no. 2, pp. 592–597, 2011.

[13] L. Ming, X. Xi, and J. Liu, "Electrochemically platinized carbon paste enzyme electrodes: a new design of amperometric glucose biosensors," *Biotechnology Letters*, vol. 28, no. 17, pp. 1341–1345, 2006.

[14] J. Kua and W. A. Goddard, "Oxidation of methanol on 2nd and 3rd row group VIII transition metals (Pt, Ir, Os, Pd, Rh, and Ru): application to direct methanol fuel cells," *Journal of the American Chemical Society*, vol. 121, no. 47, pp. 10928–10941, 1999.

[15] T. Bligaard, J. K. Nørskov, S. Dahl, J. Matthiesen, C. H. Christensen, and J. Sehested, "The Brønsted-Evans-Polanyi relation and the volcano curve in heterogeneous catalysis," *Journal of Catalysis*, vol. 224, no. 1, pp. 206–217, 2004.

[16] J. Greeley, J. Rossmeisl, A. Hellman, and J. K. Nørskov, "Theoretical trends in particle size effects for the oxygen reduction reaction," *Zeitschrift fur Physikalische Chemie*, vol. 221, no. 9-10, pp. 1209–1220, 2007.

[17] M. Lischka, C. Mosch, and A. Groß, "Tuning catalytic properties of bimetallic surfaces: oxygen adsorption on pseudomorphic Pt/Ru overlayers," *Electrochimica Acta*, vol. 52, no. 6, pp. 2219–2228, 2007.

[18] Q. Ge, S. Desai, M. Neurock, and K. Kourtakis, "CO adsorption on Pt-Ru surface alloys and on the surface of Pt-Ru bulk alloy," *The Journal of Physical Chemistry B*, vol. 105, no. 39, pp. 9533–9536, 2001.

[19] M. Gsell, P. Jakob, and D. Menzel, "Effect of substrate strain on adsorption," *Science*, vol. 280, no. 5364, pp. 717–720, 1998.

[20] P. Jakob, M. Gsell, and D. Menzel, "Interactions of adsorbates with locally strained substrate lattices," *Journal of Chemical Physics*, vol. 114, no. 22, pp. 10075–10085, 2001.

[21] Y. Shimazaki, Y. Kobayashi, S. Yamada, T. Miwa, and M. Konno, "Preparation and characterization of aqueous colloids of Pt-Ru nanoparticles," *Journal of Colloid and Interface Science*, vol. 292, no. 1, pp. 122–126, 2005.

[22] S. A. Wring and J. P. Hart, "Chemically modified, carbon-based electrodes and their application as electrochemical sensors for the analysis of biologically important compounds A review," *The Analyst*, vol. 117, no. 8, pp. 1215–1229, 1992.

[23] M. Watanabe, Y. Furuuchi, and S. Motoo, "Electrocatalysis by ad-atoms. Part XIII. Preparation of ad-electrodes with tin ad-atoms for methanol, formaldehyde and formic acid fuel cells," *Journal of Electroanalytical Chemistry*, vol. 191, no. 2, pp. 367–375, 1985.

[24] C. J. McNeil, D. Athey, and W. O. Ho, "Direct electron transfer bioelectronic interfaces: application to clinical analysis," *Biosensors and Bioelectronics*, vol. 10, no. 1-2, pp. 75–83, 1995.

[25] J. C. Claussen, A. D. Franklin, A. U. Haque, D. M. Porterfield, and T. S. Fisher, "Electrochemical Biosensor of nanocube-augmented carbon nanotube networks," *ACS Nano*, vol. 3, no. 1, pp. 37–44, 2009.

[26] S. B. Hall, E. A. Khudaish, and A. L. Hart, "Electrochemical oxidation of hydrogen peroxide at platinum electrodes. Part 1. An adsorption-controlled mechanism," *Electrochimica Acta*, vol. 43, no. 5-6, pp. 579–588, 1998.

[27] S. B. Hall, E. A. Khudaish, and A. L. Hart, "Electrochemical oxidation of hydrogen peroxide at platinum electrodes. Part II: effect of potential," *Electrochimica Acta*, vol. 43, no. 14-15, pp. 2015–2024, 1998.

[28] S. B. Hall, E. A. Khudaish, and A. L. Hart, "Electrochemical oxidation of hydrogen peroxide at platinum electrodes. Part III: effect of temperature," *Electrochimica Acta*, vol. 44, no. 14, pp. 2455–2462, 1999.

[29] S. B. Hall, E. A. Khudaish, and A. L. Hart, "Electrochemical oxidation of hydrogen peroxide at platinum electrodes. Part IV: phosphate buffer dependence," *Electrochimica Acta*, vol. 44, no. 25, pp. 4573–4582, 1999.

[30] S. B. Hall, E. A. Khudaish, and A. L. Hart, "Electrochemical oxidation of hydrogen peroxide at platinum electrodes. Part V: inhibition by chloride," *Electrochimica Acta*, vol. 45, no. 21, pp. 3573–3579, 2000.